

Classroom



In this section of *Resonance*, we invite readers to pose questions likely to be raised in a classroom situation. We may suggest strategies for dealing with them, or invite responses, or both. “Classroom” is equally a forum for raising broader issues and sharing personal experiences and viewpoints on matters related to teaching and learning science.

Understanding DC Motors through Experiments

We present here a set of simple experiments through which various characteristics of a DC motor can be investigated. The experiments also provide insights on how to control a DC motor. We first study the back-emf versus angular speed and the torque versus current characteristics. We then extract the moment of inertia of the rotor and the speed–torque curve for the load from the start-stop dynamics of the motor. Finally, we study an alternate way of obtaining the angular speed from the back-emf waveform.

1. Introduction

A three-pole DC motor is commonly used in many simple machines to convert electrical energy into mechanical energy. Such a motor consists of a stator and a rotor. The stator comprises of permanent magnets which provide a steady magnetic field and a pair of brushes as shown in *Figure 1*. The brushes are marked with the signs – and +, corresponding to the terminals of the power supply to which they are connected. The rotor comprises of three coils (wound around three poles

Harish Ravi¹ and
Rajesh B Khaparde²

¹Department of Electrical
Engineering, IIT Madras
Chennai 600036, India.
Email:
harish.ravishankar@gmail.com

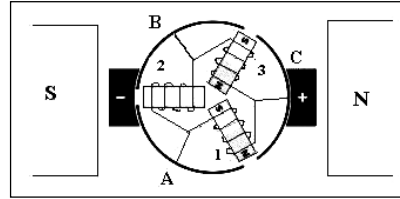
²Homi Bhabha Centre for Sci-
ence Education
TIFR VN Purav Marg, Mankhurd
Mumbai 400088, India.
Email:
rajeshkharde@gmail.com

Keywords

DC motor, motor constant, mo-
tor speed control, speed–torque
curve, start-stop dynamics.



Figure 1. Schematic diagram to illustrate the construction of a three-pole DC motor.



labeled 1, 2 and 3), a commutator ring having three segments labeled A, B and C and an axle.

At the instant shown in *Figure 1*, current passes through the coils 1 and 3 to produce a clockwise torque due to repulsion of coil 1 and attraction of coil 3 by the right (N side) magnet. Coil 2 is short-circuited by the left-hand brush. Thus the rotor rotates clockwise and a little while later, the current passes through all the three coils and the rotor continues to rotate clockwise. The interconnection of the coils to the commutator segments is in such a way that the torque produced by the rotor is always in the same direction [1].

2. Theoretical Analysis

2.1 Basic Equations for a DC Motor

When the rotor rotates in the presence of a steady magnetic field, a back-emf E_b is generated across the rotor coils in accordance with Faraday's law and is expected to be linearly proportional to the angular speed ω (henceforth called speed) of the rotor. Thus, we can write

$$E_b = k_1 \omega , \tag{1}$$

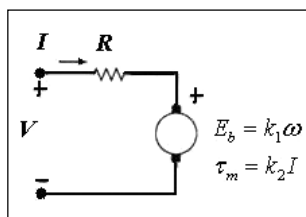
where k_1 is a constant.

A motor can be represented as a source of emf E_b connected in series with its resistance R as shown in *Figure 2*.

Applying Kirchoff's voltage law, we obtain

$$I = \frac{V - E_b}{R} , \tag{2}$$

Figure 2. Equivalent circuit representation of a DC motor.



where I is the current passing through the motor and V is the voltage applied across the motor. Lorentz force law dictates that the motor torque τ_m is expected to be linearly proportional to the current I passing through the motor. That is,

$$\tau_m = k_2 I, \quad (3)$$

where k_2 is a constant. The conservation of power gives $k_1 = k_2 = k_m$, where k_m is called the motor constant.

2.2 Speed–Torque Curve

A speed–torque curve (henceforth called s – t curve) is a graph showing variation of torque with speed. The s – t curve for a DC motor should be a straight line. We can obtain the relation between motor torque τ_m and the speed ω using (1), (2) and (3):

$$\tau_m = \frac{k_m V}{R} - \frac{k_m^2}{R} \omega. \quad (4)$$

A torque that opposes the motor torque is often called the load torque τ_{load} . It is usually frictional and can be considered as a static torque τ_s plus a viscous component $b\omega$.

$$\tau_{\text{load}} = \tau_s + b\omega. \quad (5)$$

Thus, the motor torque decreases with increasing speed while the load torque increases with increasing speed. The motor operates at the point of intersection of the s – t curves for the load and the motor as illustrated later in *Figure 3*.

2.3 Start–Stop Dynamics

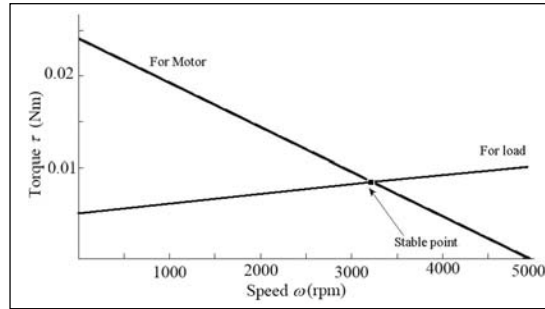
Let us understand the dynamics of starting of a motor. If J indicates the moment of inertia of the rotor, then the law of rotation gives,

$$\tau_m - \tau_{\text{load}} = J\alpha, \quad (6)$$

The motor torque decreases with increasing speed while the load torque increases with increasing speed.



Figure 3. s–t curves for the motor and the load.



where α is the angular acceleration (henceforth called acceleration) of the rotor. Substituting for the torques from (4) and (5), and assuming a constant voltage source, we can write,

$$\frac{k_m(V - k_m\omega)}{R} - \tau_s - b\omega = J \frac{d\omega}{dt} . \quad (7)$$

After integrating (7), we obtain an exponentially increasing function for speed ω . Thus, the back-emf increases with time and from (2), it follows that the current should exponentially decrease. In a hypothetical situation, when a motor has zero load and is driven by a constant voltage power supply, the rotor would speed up to the point where the back-emf equals the voltage applied across the motor and hence the current would fall to zero.

In a hypothetical situation, when a motor has zero load and is driven by a constant voltage power supply, the rotor would speed up to the point where the back-emf equals the voltage applied across the motor and hence the current would fall to zero.

Now, let us understand the dynamics of stopping of a motor. When the power supply is disconnected, only the load torque τ_{load} is responsible for slowing down the rotor and hence we can write,

$$\tau_{load} = \tau_s + b\omega = -J \frac{d\omega}{dt} . \quad (8)$$

After integrating (8), we note that the speed ω should fall exponentially with time. One can stop the rotor quicker by shorting the motor terminals and thereby allowing current to pass through the rotor coils which produces an opposing torque in accordance with Lenz’s law.



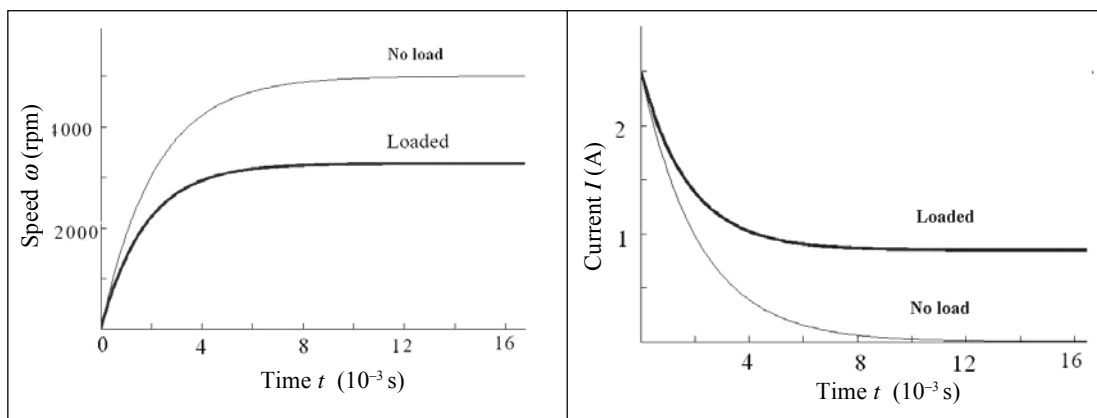


Figure 4. Graphs of speed versus time and current versus time for starting.

To illustrate the above, we simulated the $s-t$ curve and the start-stop dynamics obtained by solving the above equations. We used $k_m = 9.65 \times 10^{-3}$ Vs, $R = 2$, $J = 10^{-7}$ kgm², $b = 10^{-5}$ Nms and $\tau_s = 0.005$ Nm.

Here, note that the steady-state speed in the loaded case (Figure 4) is close to that obtained at the point of intersection of $s-t$ curves for the load and the motor (Figure 3). Also note that the no load steady-state speed (Figure 4) matches with that obtained from the $s-t$ curve (Figure 3) for the motor at the point of intersection with the X-axis. The time constants for the speed versus time curve and the current versus time curve obtained from the formulae were both equal to 2.1 ms.

2.4 Analysis of Back-Emf Waveform

Though the back-emf waveform should be an average DC, it has a small AC component due to the commutator brush arrangement and also due to the changing angle of the rotor coils with respect to the magnetic field. There would be sharp dips due to loss of contact at the gaps of the commutator or due to shorting of one of the coils. If there are p poles, there would be p gaps between the commutator segments as indicated in Figure 1. Each gap would pass over each brush once in a rotation. As there are two brushes, there will be two dips in the voltage waveform due to each gap and

Though the back-emf waveform should be an average DC, it has a small AC component due to the commutator brush arrangement and also due to the changing angle of the rotor coils with respect to the magnetic field.



The frequency of dips would reveal the number of poles in the motor and could also be used to find the speed of the rotor.

hence, the frequency f of the dips should be,

$$f = 2p\omega. \quad (9)$$

Thus, the frequency of dips would reveal the number of poles in the motor and could also be used to find the speed of the rotor.

3. Experimental Study

In this investigation, we used two similar DC motors, one was named as the test motor and the other was called the drive motor. A variable DC power supply was used to provide the necessary power to the motors and a non-contact type digital tachometer was employed to measure the speed of the rotor.

3.1 Back-Emf–Speed Relation

The test motor was clamped to a retort stand and run at different speeds by varying the voltage of the power supply. For various voltages, the speed was measured using the tachometer. The resistance R of the motor was initially measured using a multimeter. The back-emf was calculated from measured values of V and I using (3). The back-emf versus speed was then plotted and the value of motor constant k_m was determined.

3.2 Torque–Current Relation

A motor coupled to a pulley with a known radius was clamped to a retort stand. A set of slotted masses was attached to a string wound around the pulley and was held suspended as shown in *Figure 5*. The current passing through the motor (which caused an opposing torque) was increased until the mass just moved down upon releasing. Thus the balancing point was determined and the motor torque was counter-balanced by the torque due to the mass. The current versus mass curve was plotted to understand the current–torque relationship.



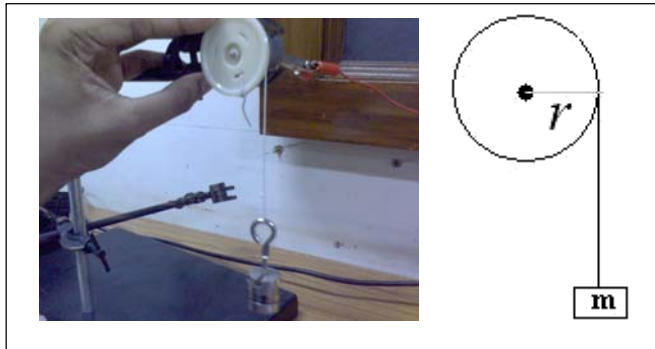


Figure 5. The arrangement of mass hung from the pulley.

3.3 Start-Stop Dynamics

Since the first experiment established the relationship between back-emf and angular speed, we exploited it to measure the transient rotational response of the motor. The back-emf was calculated from the current which was measured using a small series resistance (*Figure 6*). The motor was powered using a constant voltage source and the transient voltage curve across the series resistance was monitored on a storage oscilloscope. This curve gave information about the start dynamics as it revealed the speed at every time instant. The stop dynamics however, was obtained more easily as the back-emf was directly available across the motor terminals while stopping. The speed–time curves obtained can then be differentiated to obtain instantaneous accelerations. A RC filtering circuit was used to filter out the spikes in the voltage waveform due to commutations. These commutations were actually used in the next experiment to measure speed. One must note that the moment of inertia of the rotor can be obtained only by studying the dynamics.

The motor was powered using a constant voltage source and the transient voltage curve across the series resistance was monitored on a storage oscilloscope.

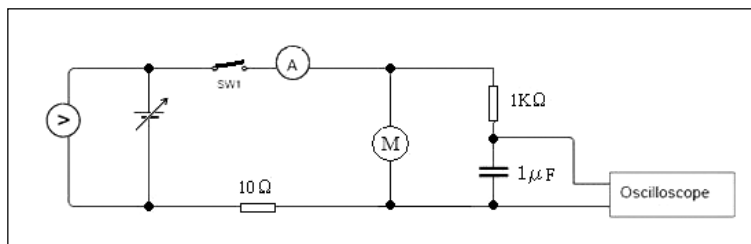


Figure 6. Circuit diagram for studying the stopping back-emf curve.



The moment of inertia of the rotor can be calculated from the initial acceleration and the steady-state current before disconnecting the power supply.

3.3.1 Stop Dynamics: Suppose a running motor is disconnected from a power supply at $t = 0$. Just before disconnecting the power supply (i.e., $t = 0^-$), the rotor was in steady state, which means the motor torque τ_m was balancing the load torque τ_{load} . Thus, we can write,

$$k_m I_{t=0^-} = \tau_{load} . \quad (10)$$

At an instant immediately after disconnecting the power supply (i.e., $t = 0^+$), the speed would not have changed and thus, τ_{load} which was responsible for the initial deceleration also would not have changed. Thus, we can write,

$$\tau_{load} = -J\alpha_{t=0^+} , \quad (11)$$

$$k_m I_{t=0^-} = -J\alpha_{t=0^+} . \quad (12)$$

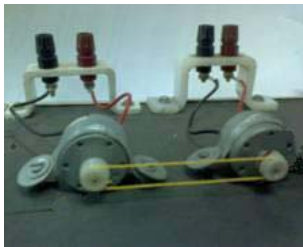
Hence, the moment of inertia J of the rotor can be calculated from the initial acceleration (actually deceleration) and the steady-state current before disconnecting the power supply using (12). The load torque at each instant can then be calculated from the acceleration and then, the $s-t$ curve can be plotted for the load.

3.3.2 Start Dynamics: The start dynamics was obtained by monitoring the voltage V_{sr} across a small known series resistance. At any time instant while starting,

$$k_m I - \tau_{load} = J\alpha \quad (13)$$

Using the moment of inertia found in the previous experiment, the load torque τ_{load} can be calculated at each instant from the acceleration and current using (13) and then, the $s-t$ curve can be plotted for the load.

Figure 7. Photograph of the coupled motors to study back-emf waveform.



3.4 Analysis of Back-Emf Waveform

A drive motor and a test motor were coupled using a belt and two identical pulleys as shown in *Figure 7*. The drive motor was connected to a variable DC power supply and was used to control the speed of the system. The



back-emf waveform of the test motor was monitored on an oscilloscope for different speeds which were measured using a non-contact type tachometer. The frequency of the back-emf waveform was plotted against the measured speed.

4. Results and Discussion

We studied the characteristics of four DC motors (a 7-pole, a 5-pole and two 3-pole motors) and obtained consistent results which complemented the theoretical predictions. We present below our observations and results recorded for a 5-pole DC motor.

4.1 Back-Emf–Speed Relation

We obtained a straight line passing through the origin for the back-emf versus speed graph as shown in *Figure 8*, whose slope gave $k_m = 2.32 \times 10^{-3} \text{V/rpm} = 2.22 \times 10^{-2} \text{Vs}$, and thus verified that the back-emf is indeed linearly proportional to the speed as expected from Faraday’s law.

4.2 Torque–Current Relation

We obtained a straight line for the current–mass graph which experimentally confirmed that the torque produced by the rotor is linearly proportional to the current passing through the motor as expected from Lorentz law

$$\tau_m = k_m I = -\tau_s + mgr. \quad (14)$$

We studied the characteristics of four DC motors and obtained consistent results which complemented the theoretical predictions.

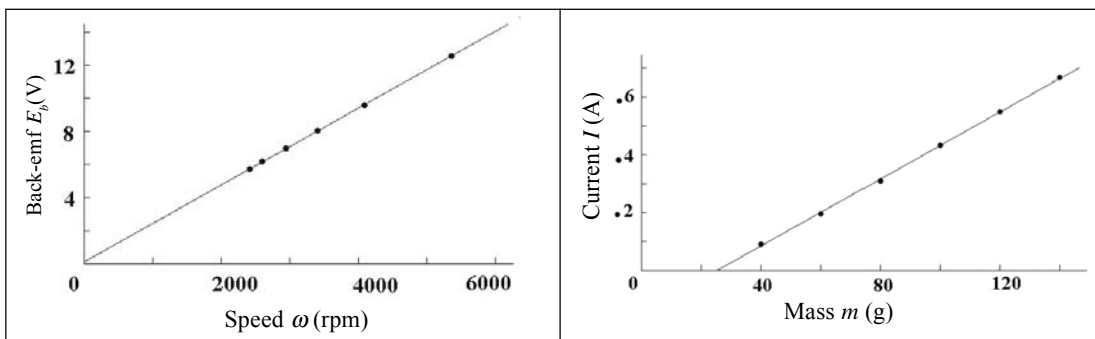


Figure 8.(left) A graph of back-emf versus speed. Figure 9. (right) A graph of current versus mass.



The stopping back-emf waveform looks linear near the end where the static frictional torque dominates and causes a uniform deceleration.

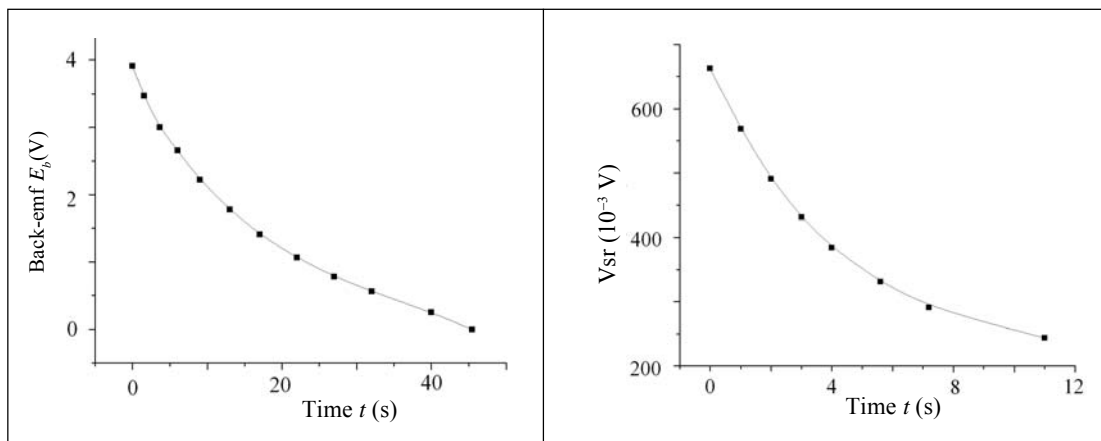
We obtained $k_m = 2.26 \times 10^{-2}$ Nm/A and the static frictional torque $\tau_s = 3.42 \times 10^{-3}$ Nm. We wish to draw attention to the fact that the value of the motor constant k_m obtained here is consistent with that obtained from the back-emf–speed graph. Note that we would have obtained a positive intercept in the current–mass graph if we had measured the current required for the masses to just lift off the surface.

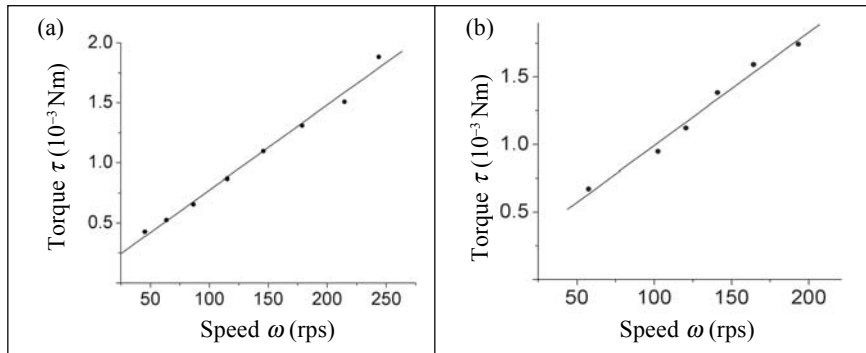
4.3 Start–Stop Dynamics

This experiment was performed with a different DC motor. We obtained the exponential graphs for stopping and starting as shown in *Figures 10* and *11*, respectively. Note that the stopping back-emf waveform looks linear near the end where the static frictional torque dominates and causes a uniform deceleration.

The moment of inertia J of the rotor was calculated to be 1.3×10^{-4} kgm² from the initial deceleration and the steady-state current before disconnecting the power supply. At each instant, the speed ω was calculated from the back-emf and the acceleration α was determined from the slope of the back-emf versus time graph. Also, the load torque τ_{load} was calculated from the acceleration as described earlier and the s – t curve for the load was plotted for stopping and starting as shown in *Figure 12*.

Figure 10.(left) Back-emf versus time for stopping. Figure 11. (right) Voltage Vsr versus time for starting.





Note that there is a considerable error in the value of the torque calculated due to inaccuracies in the determination of slope, motor constant and moment of inertia. One may obtain more reliable results using a computer-interfaced data-acquisition system.

Figure 12. $s-t$ curves for the load obtained from (a) stopping and (b) starting.

4.4 Analysis of Back-Emf Waveform

We observed a back-emf waveform as shown in *Figure 13*. The amplitude of the waveform was much smaller than the average DC which was blocked. The waveform had a periodic alternate repeating pattern. The adjacent dips were due to two different brushes while the alternate dips were due to the same brush. The adjacent dips look different due to a slight asymmetry in the brushes.

The graph of frequency of the back-emf waveform versus speed of the rotor turned out to be a straight line as shown in *Figure 14*. The slope of the straight line gave $2p = 10.07$, which was very close to the expected value of 10, as the motor had five poles.

The adjacent dips were due to two different brushes while the alternate dips were due to the same brush. The adjacent dips look different due to a slight asymmetry in the brushes.

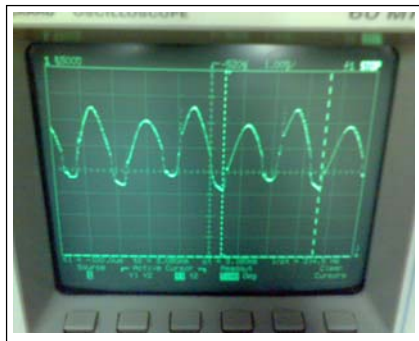
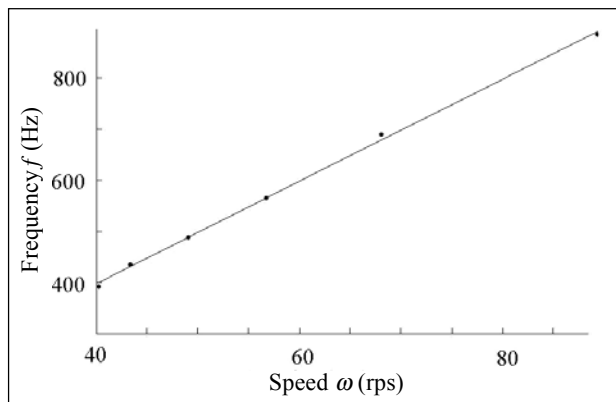


Figure 13. Photograph of back-emf waveform observed on a storage oscilloscope.



Figure 14. A graph of frequency versus speed.



5. Conclusions

We have demonstrated a set of simple experiments through which the fundamental characteristics, like back-emf–speed, and torque–current relationships of a DC motor were experimentally confirmed. We then used the back-emf–speed relation to examine the transient rotational response of the rotor while starting and stopping. From this, we obtained the moment of inertia of the rotor and the load s – t curve. Finally, we studied an alternate method of measuring the angular speed of the rotor from the commutation dips. We suggest that this set of simple experiments may be tried out in an undergraduate teaching laboratory for physics and electrical engineering students.

Suggested Reading

- [1] <http://www.stefanv.com/rcstuff/qf200212.html>
- [2] Exp Test 2-B, *Indian National Physics Olympiad, OCSC, HBCSE, 2003.*
- [3] Fitzgerald, *Electric Machinery*, McGraw Hill, 2003.
- [4] R L Weber, K V Manning et al, *College Physics*, 5th edition, Tata McGraw Hill, 1995.

Acknowledgements

We are grateful to Profs. Arvind Kumar, Vijay Singh and H C Pradhan for providing the necessary support and facilities for this study under the NIUS programme. We are also extremely thankful to Profs. M L Ogala-purkar and D A Desai for the initial development, support and for motivating us to take up the study. We appreciate the help and support received from the project staff of the physics laboratories at HBCSE.

